

# Tethered trinuclear cyclometalated platinum(II) complexes: from crystal engineering to tunable emission energy†

Wei Lu, Nianyong Zhu and Chi-Ming Che\*

Department of Chemistry and the HKU-CAS Joint Laboratory on New Materials, The University of Hong Kong, Pokfulam Road, Hong Kong SAR, China. E-mail: cmche@hku.hk

Received (in Cambridge, UK) 22nd January 2002, Accepted 7th March 2002

First published as an Advance Article on the web 26th March 2002

The crystal structures and photoluminescence of trinuclear cyclometalated platinum(II) complexes are dependent on the tethering phosphine ligands and sensitive to metal–metal contacts and  $\pi$ – $\pi$  stacking interactions.

Cyclometalated and oligopyridine  $d^8$  metal complexes have recently been shown to have useful applications in materials science and chemosensings.<sup>1–5</sup> The  $[(C^{\wedge}N^{\wedge}N)Pt]^+$  ( $HC^{\wedge}N^{\wedge}N = 6$ -aryl-2,2'-bipyridine) luminophores<sup>2</sup> have the combined structural and spectroscopic features of both cyclometalated and bipyridine Pt(II) complexes, and are better visible-light emitters than their terpyridine<sup>3</sup> and  $C^{\wedge}N^{\wedge}C$  ( $HC^{\wedge}N^{\wedge}CH = 2,6$ -diphenylpyridine)<sup>4</sup> congeners. We previously noted that the photoluminescent properties of  $[(C^{\wedge}N^{\wedge}N)_2Pt_2]^{n+}$  complexes with bridging phosphine or pyrazole ligands are affected by weak metal–metal and ligand–ligand interactions which are sensitive to the micro-environment.<sup>5</sup> We conceive that allosteric and cooperative effects arising from molecular interactions of more than two  $[(C^{\wedge}N^{\wedge}N)Pt]^+$  moieties could lead to novel class of sensory materials with visible emission as the reporter signal.

Four trinuclear  $[(C^{\wedge}N^{\wedge}N)_3Pt_3(\mu_3-L)]^{3+}$  ( $HC^{\wedge}N^{\wedge}N = 6$ -phenyl-2,2'-bipyridine,  $L = 1,1,1$ -tris(diphenylphosphino-methyl) ethane (tpe), **1**;  $L =$  bis(diphenylphosphino-methyl)phenylphosphine (dpmp), **2**;  $HC^{\wedge}N^{\wedge}N = 4$ -(*p*-MeOC<sub>6</sub>H<sub>4</sub>)-6-phenyl-2,2'-bipyridine,  $L =$  dpmp, **3**;  $HC^{\wedge}N^{\wedge}N = 6$ -(2-thienyl)-2,2'-bipyridine,  $L =$  dpmp, **4**) complexes were prepared by treating  $[(C^{\wedge}N^{\wedge}N)PtCl]$  with the phosphine ligands (schematic drawings in ESI†).

The crystal structure of **1**(ClO<sub>4</sub>)<sub>3</sub> (Fig. 1)‡ reveals a propeller-shape cation consisting of three  $[(C^{\wedge}N^{\wedge}N)Pt]^+$  units arranged around the tpe ligand with a  $C_{3v}$  symmetry. No intra- or intermolecular Pt–Pt and  $\pi$ – $\pi$  contacts ( $< 4$  Å) are observed. Instead, C–H... $\pi$  interactions (indicated by the short contacts between H28 and H23 and carbon atoms of the  $C^{\wedge}N^{\wedge}N$  ligands,  $\sim 3.0$  Å) are discerned, which are mandatory to keep the rigid shape of the complex cation.‡

In contrast, complex **2**(ClO<sub>4</sub>)<sub>3</sub> crystallises in four different forms with various colour, depending upon the conditions of crystallisation. A perspective view of the cation in the red form of **2**(ClO<sub>4</sub>)<sub>3</sub>·H<sub>2</sub>O,‡ obtained by slow diffusion of benzene into acetonitrile solution, is shown in Fig. 2. This structure consists of three  $[(C^{\wedge}N^{\wedge}N)Pt]^+$  units tethered into a linear shape by the dpmp ligand. The three planar  $[(C^{\wedge}N^{\wedge}N)Pt]^+$  units are virtually parallel to each other but staggered with torsion angles of 26 and 16° about the Pt1–Pt2 and Pt2–Pt3 axis respectively (defined by the angle between the Pt1–Pt2–N2 and Pt1–Pt2–N4 planes, and between the Pt2–Pt3–N2 and Pt2–Pt3–N6 planes, respectively). The Pt1–Pt2 and Pt2–Pt3 distances of 3.19 and 3.40 Å, respectively, together with the Pt1–Pt2–Pt3 angle of 169° reveal that there exists weak metal–metal interactions among the three Pt atoms. Upon diffusion of diethyl ether into acetonitrile solution of **2**(ClO<sub>4</sub>)<sub>3</sub>, three crystal forms with colour being yellow, orange and red were obtained.‡ The red form was resolved by X-ray crystallography to be identical to the one

† Electronic supplementary information (ESI) available: schematic drawings for **1–4**, perspective view of cation of **4**(ClO<sub>4</sub>)<sub>3</sub>·1.5Et<sub>2</sub>O·CH<sub>3</sub>CN and refinement details for X-ray crystallography. See <http://www.rsc.org/suppdata/cc/b2/b200723a/>

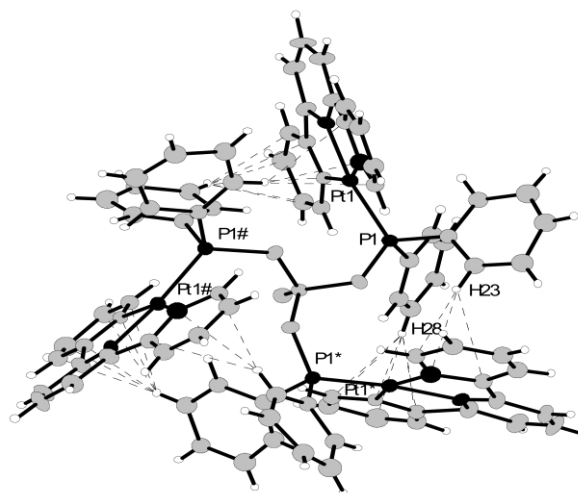


Fig. 1 Perspective view of the cation of **1**(ClO<sub>4</sub>)<sub>3</sub> with dashed lines indicating C–H... $\pi$  contacts ( $< 3.12$  Å).

depicted above. The yellow and orange forms change immediately into red form upon retrieved from the mother liquor. Crystals of the orange form (**2**(ClO<sub>4</sub>)<sub>3</sub>·2Et<sub>2</sub>O·CH<sub>3</sub>CN) were obtained and its structure is shown in Fig. 3. The three planar  $[(C^{\wedge}N^{\wedge}N)Pt]^+$  are staggered with torsion angles of 35 and 5° about the Pt1–Pt2 and Pt2–Pt3 axis respectively. The intramolecular metal–metal separations are Pt1–Pt2, 3.36 and Pt2–Pt3, 3.62 Å and the Pt1–Pt2–Pt3 angle is 162°. There exist weak metal–metal interaction between Pt1 and Pt2 but not Pt2 and Pt3, for the Pt2–Pt3 separation of 3.62 Å is beyond the range of intermetal distances (3.09–3.50 Å) observed in monomeric Pt(II) extended linear-chain structures.<sup>6</sup> In the crystal lattice, two complex cations of **2** are packed into a slightly off-set head-to-tail pair by  $\pi$ – $\pi$  stacking interactions ( $\pi$ – $\pi$  separation  $\sim 3.5$  Å). The crystallisation of complex **2** depends on the counter anions. For **2**(BF<sub>4</sub>)<sub>3</sub>, an orange form was found in the mother liquor which turned red upon collection on the sinter glass. For **2**(PF<sub>6</sub>)<sub>3</sub>, only a red-coloured crystalline solid was found. After standing, the red form of these solids slowly turned brown-red, presumably due to lattice contraction induced by lost of solvated molecules. No polymorphism was observed for **3**(ClO<sub>4</sub>)<sub>3</sub> and **4**(ClO<sub>4</sub>)<sub>3</sub> crystals which are brown red in colour.

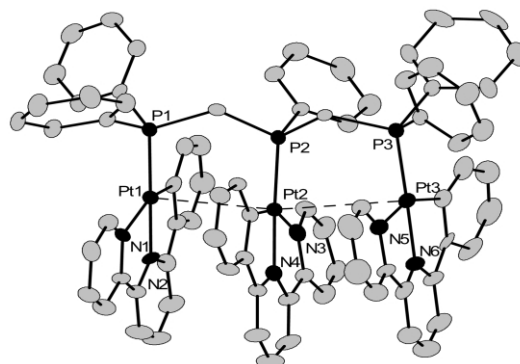
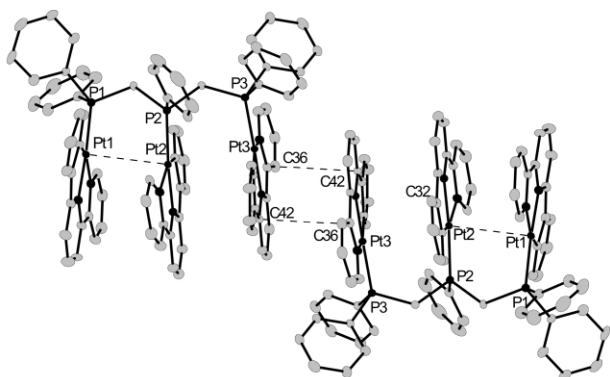


Fig. 2 Perspective view of the cation of the red form **2**(ClO<sub>4</sub>)<sub>3</sub>·H<sub>2</sub>O.



**Fig. 3** View of a pair of cations of orange form  $2(\text{ClO}_4)_3 \cdot 2\text{Et}_2\text{O} \cdot \text{CH}_3\text{CN}$  with dashed lines indicating contacts shorter than sum of van der Waal radii.

The crystal structure of  $4(\text{ClO}_4)_3 \cdot 1.5\text{Et}_2\text{O} \cdot \text{CH}_3\text{CN}$  (see ESI†) reveals weak intramolecular metal–metal contacts (Pt1–Pt2 3.25, Pt2–Pt3 3.39 Å).

A correlation between crystal structure and solid-state emission (Fig. 4) is made. The green yellow emission ( $\lambda_{\text{max}} = 544 \text{ nm}$ ,  $\tau = 5.9 \mu\text{s}$ ) from the  $1(\text{ClO}_4)_3$  solid is blue-shifted from the  $^3\text{MLCT}$  emission ( $\sim 560 \text{ nm}$ ) of the  $[(\text{C}^{\wedge}\text{N}^{\wedge}\text{N})\text{Pt}(\text{PPh}_3)]^+$  salt in acetonitrile.<sup>2</sup> This is ascribed to the C–H $\cdots\pi$  interactions found in the crystal lattice of  $1(\text{ClO}_4)_3$ . The emission ( $\lambda_{\text{max}} = 630 \text{ nm}$ ,  $\tau = 1.5 \mu\text{s}$ ) from the orange form of **2** compares well with the emission energy of  $[(\text{C}^{\wedge}\text{N}^{\wedge}\text{N})_2\text{Pt}_2(\mu\text{-dppm})]^{2+}$  salt,<sup>5</sup> thus the former is similarly assigned to a  $^3(\pi\pi^*)$  excimer with  $^3\text{MMLCT}$  character; this accords to the fact that there is only one pair of Pt–Pt contact  $< 3.5 \text{ \AA}$  and the packing of the orange form is dominated by intermolecular  $\pi$ – $\pi$  interaction. The red emissions [ $\lambda_{\text{max}} = 674 (0.9 \mu\text{s})$ ,  $709 (0.4 \mu\text{s}) \text{ nm}$ , respectively] from the red and brown red forms of **2** are seldom encountered in luminescent cyclometalated Pt(II) complexes.<sup>5,7</sup> Recently, we assigned the 710 nm emission from an acetonitrile solution of  $[(\text{C}^{\wedge}\text{N}^{\wedge}\text{N})\text{Pt}(\text{C}\equiv\text{NR})]^+$  salt with concentration  $\geq 7 \times 10^{-3} \text{ mol dm}^{-3}$  to be  $^3\text{MMLCT}$  in nature.<sup>7</sup> The emission from the yellow crystalline form **2** cannot be accurately recorded due to rapid loss of solvated molecules.

The UV-vis spectra of  $2(\text{ClO}_4)_3$ – $4(\text{ClO}_4)_3$  in acetonitrile at 298 K (Fig. 5) feature broad absorption in the range of 400–600 nm with average  $\epsilon$  value being  $\sim 5000 \text{ dm}^3 \text{ mol}^{-1} \text{ cm}^{-1}$ , which are more intense than that in the binuclear analogue  $[(\text{C}^{\wedge}\text{N}^{\wedge}\text{N})_2\text{Pt}_2(\mu\text{-dppm})](\text{ClO}_4)_2$  and are comparable to the  $^1\text{MLCT}$  absorption of classical  $[\text{Ru}(\alpha\text{-diimine})_3]^{2+}$  salts. The lowest-energy allowed transitions at 517 and 522 nm for  $2(\text{ClO}_4)_3$  and  $3(\text{ClO}_4)_3$  respectively, are assigned as  $^1\text{MMLCT}$  in nature, after our recent study on  $[(\text{C}^{\wedge}\text{N}^{\wedge}\text{N})\text{Pt}(\text{C}\equiv\text{NR})]^+$  salts.<sup>7</sup> These low-energy transitions are not observed in the UV-vis spectrum of  $1(\text{ClO}_4)_3$  where short intramolecular Pt–Pt and  $\pi$ – $\pi$  contacts are not possible due to the propeller shape of the molecule. The emission energies of  $1(\text{ClO}_4)_3$ – $4(\text{ClO}_4)_3$  [ $\lambda_{\text{max}} =$

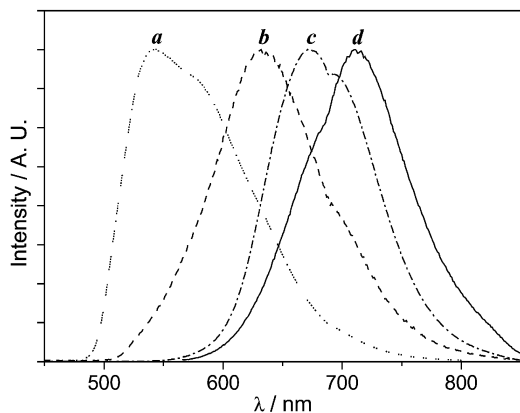


**Fig. 4** Solid-state emission spectra of (a)  $1(\text{ClO}_4)_3$ , (b) orange  $2(\text{BF}_4)_3$ , (c) red, and (d) brown-red form of  $2(\text{ClO}_4)_3$  at 298 K.

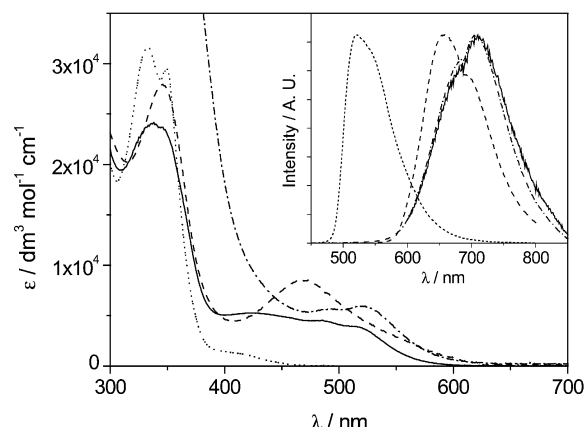


**Fig. 5** UV-vis and normalised emission (inset) spectra of  $1(\text{ClO}_4)_3$  (···),  $2(\text{ClO}_4)_3$  (—),  $3(\text{ClO}_4)_3$  (---) and  $4(\text{ClO}_4)_3$  (-·-) in acetonitrile at 298 K.

520 (8.0  $\mu\text{s}$ ), 710 (= 0.1  $\mu\text{s}$ ), 710 (1.0  $\mu\text{s}$ ), 657 (1.3  $\mu\text{s}$ ) nm, respectively] in acetonitrile at 298 K (Fig. 5, inset) compare well with those observed in solid forms, thus the propeller and linear configuration are kept in fluid solutions respectively.

In summary, the absorption and emission energies of oligomeric cyclometalated Pt(II) complexes can be tuned to a large extent by choosing the tethering phosphine ligands. It is envisaged that chemosensors based on this class of luminophores are potential amplifiers for subtle signal inputs.

We are grateful for financial support from the Hong Kong University Foundation and the Research Grants Council of Hong Kong SAR, China [HKU 7298/99].

## Notes and references

‡ Crystal data for  $1(\text{ClO}_4)_3$ :  $\text{C}_{89}\text{H}_{72}\text{Cl}_3\text{N}_6\text{O}_{12}\text{P}_3\text{Pt}_3$ ,  $M = 2202.06$ , hexagonal,  $P6_3/m$ ,  $a = 14.536(2)$ ,  $c = 23.211(5) \text{ \AA}$ ,  $\gamma = 120^\circ$ ,  $V = 4247.3 \text{ \AA}^3$ ,  $Z = 2$ ,  $D_c = 1.722 \text{ g cm}^{-3}$ ,  $\mu(\text{Mo-K}\alpha) = 5.14 \text{ mm}^{-1}$ ,  $F(000) = 2148$ , 2733 independent reflections,  $R_1 = 0.053$  ( $I > 2\sigma(I)$ ),  $wR_2 = 0.145$ ,  $\text{GOF}(F^2) = 1.096$ . For  $2(\text{ClO}_4)_3 \cdot \text{H}_2\text{O}$ :  $\text{C}_{80}\text{H}_{64}\text{Cl}_3\text{N}_6\text{O}_{13}\text{P}_3\text{Pt}_3$ ,  $M = 2101.90$ , monoclinic,  $P2_1/c$ ,  $a = 15.592(3)$ ,  $b = 12.671(3)$ ,  $c = 38.474(8) \text{ \AA}$ ,  $\beta = 92.92(3)^\circ$ ,  $V = 7591(3) \text{ \AA}^3$ ,  $Z = 4$ ,  $D_c = 1.839 \text{ g cm}^{-3}$ ,  $\mu(\text{Mo-K}\alpha) = 5.75 \text{ mm}^{-1}$ ,  $F(000) = 4080$ , 10070 independent reflections,  $R_1 = 0.049$  ( $I > 2\sigma(I)$ ),  $wR_2 = 0.120$ ,  $\text{GOF}(F^2) = 0.880$ . For  $2(\text{ClO}_4)_3 \cdot 2\text{Et}_2\text{O} \cdot \text{CH}_3\text{CN}$ :  $\text{C}_{90}\text{H}_{85}\text{Cl}_3\text{N}_7\text{O}_{14}\text{P}_3\text{Pt}_3$ ,  $M = 2273.22$ , triclinic,  $P1$ ,  $a = 12.398(3)$ ,  $b = 15.449(3)$ ,  $c = 23.519(5) \text{ \AA}$ ,  $\alpha = 82.20(3)$ ,  $\beta = 89.42(3)$ ,  $\gamma = 88.49(3)^\circ$ ,  $V = 4461.4(17) \text{ \AA}^3$ ,  $Z = 2$ ,  $D_c = 1.689 \text{ g cm}^{-3}$ ,  $\mu(\text{Mo-K}\alpha) = 4.90 \text{ mm}^{-1}$ ,  $F(000) = 2224$ , 14897 independent reflections,  $R_1 = 0.043$  ( $I > 2\sigma(I)$ ),  $wR_2 = 0.112$ ,  $\text{GOF}(F^2) = 0.949$ .

CCDC reference numbers 178372–178375.

See <http://www.rsc.org/suppdata/cc/b2/b200723a/> for crystallographic data in CIF or other electronic format.

- M. Gianini, A. von Zelewsky and H. Stoeckli-Evans, *Inorg. Chem.*, 1997, **36**, 6094 and references therein; S. W. Lai, M. C. W. Chan, S. M. Peng and C. M. Che, *Angew. Chem., Int. Ed.*, 1999, **38**, 669; C. M. Che, M. S. Yang, K. H. Wong, H. L. Chan and W. Lam, *Chem. Eur. J.*, 1999, **5**, 3350; R. D. Sommer, A. L. Rheingold, A. J. Goshe and B. Bosnich, *J. Am. Chem. Soc.*, 2001, **123**, 3940; T. Yamaguchi, F. Yamazaki and T. Ito, *J. Am. Chem. Soc.*, 2001, **123**, 743; J. E. McGarrah, Y. J. Kim, M. Hissler and R. Eisenberg, *Inorg. Chem.*, 2001, **40**, 4510.
- C. W. Chan, T. F. Lai, C. M. Che and S. M. Peng, *J. Am. Chem. Soc.*, 1993, **115**, 11245; L. Z. Wu, T. C. Cheung, C. M. Che, K. K. Cheung and M. H. W. Lam, *Chem. Commun.*, 1998, 1127; F. Neve, M. Ghedini and A. Crispini, *Chem. Commun.*, 1996, 2463; W. Lu, B. X. Mi, M. C. W. Chan, Z. Hui, N. Y. Zhu, S. T. Lee and C. M. Che, *Chem. Commun.*, 2002, 206.
- G. Arena, G. Calogero, S. Campagna, L. M. Scolaro, V. Ricevuto and R. Romeo, *Inorg. Chem.*, 1998, **37**, 2763; J. F. Michalec, S. A. Bejune and D. R. McMillin, *Inorg. Chem.*, 2000, **39**, 2708.
- W. Lu, M. C. W. Chan, K. K. Cheung and C. M. Che, *Organometallics*, 2001, **20**, 2477.
- S. W. Lai, M. C. W. Chan, T. C. Cheung, S. M. Peng and C. M. Che, *Inorg. Chem.*, 1999, **38**, 4046.
- W. B. Connick, R. E. Marsh, W. P. Schaefer and H. B. Gray, *Inorg. Chem.*, 1997, **36**, 913.
- S. W. Lai, H. W. Lam, W. Lu, K. K. Cheung and C. M. Che, *Organometallics*, 2002, **21**, 226.